

# Plane wave/pseudopotential implementation of excited state gradients in density functional linear response theory: a new route via implicit differentiation

Nikos L. Doltsinis<sup>1</sup> and D. S. Kosov<sup>2</sup>

<sup>1</sup>*Lehrstuhl für Theoretische Chemie,  
Ruhr-Universität Bochum,  
D-44780 Bochum, Germany*

<sup>2</sup>*Department of Chemistry and Biochemistry,  
University of Maryland,  
College Park, MD 20742*

## Abstract

This work presents the formalism and implementation of excited state nuclear forces within density functional linear response theory (TDDFT) using a plane wave basis set. An implicit differentiation technique is developed for computing nonadiabatic coupling between Kohn-Sham molecular orbital wavefunctions as well as gradients of orbital energies which are then used to calculate excited state nuclear forces. The algorithm has been implemented in a plane wave/pseudopotential code taking into account only a reduced active subspace of molecular orbitals. It is demonstrated for the H<sub>2</sub> and N<sub>2</sub> molecules that the analytical gradients rapidly converge to the exact forces when the active subspace of molecular orbitals approaches completeness.

*J. Chem. Phys.* 122, 144101 (2005)

## I. INTRODUCTION

The past decade has seen time-dependent density functional linear response theory (TDDFT)<sup>1,2,3</sup> become the most widely used electronic structure method for calculating vertical electronic excitation energies<sup>4,5</sup>. Except for certain well-known problem cases such as, for instance, charge transfer<sup>6,7,8</sup> and double excitations<sup>9</sup>, TDDFT excitation energies are generally remarkably accurate, typically to within a fraction of an electron Volt<sup>10,11,12,13</sup>.

Excited state analytical nuclear forces within TDDFT have only been implemented recently<sup>14,15,16,17</sup> in an attempt to extend the applicability of TDDFT beyond single point calculations. One complication has been the fact that TDDFT merely provides excitation energies, but excited state wavefunctions are not properly defined. The first excited state geometry optimization using analytical gradients was presented by van Caillie and Amos based on a Handy-Schaefer Z-vector method<sup>14,15</sup>. An extended Lagrangian ansatz was chosen by Furche and Ahlrichs<sup>16</sup> and Hutter<sup>17</sup> for their Gaussian-type basis set and plane wave/pseudopotential implementations, respectively. The latter variant is of particular importance for condensed phase applications since it is used in conjunction with periodic boundary conditions. In order to ensure completeness, the number of Kohn-Sham (KS) orbitals included in constructing the response matrix in a molecular orbital (MO) basis must equal the number of basis functions. Since a plane wave basis typically consists of two orders of magnitude more basis functions than a Gaussian-type basis set a complete MO formulation of TDDFT is impractical. A solution to this problem is to cast the working matrix equations directly into a plane wave basis as proposed by Hutter<sup>17</sup>. Earlier, Doltsinis and Sprik<sup>18</sup> have proposed an alternative, *active space* approach to TDDFT in which only a subset of (active) KS orbitals is selected to construct the response matrix. For a large variety of excited states, convergence of the corresponding excitation energies has been shown to be rapid with respect to the number of orbitals included in the active space<sup>8,18</sup>. In the present paper, we shall follow this active space ansatz and derive analytical expressions for excited state nuclear forces within an MO basis. In contrast to previous work, we do not rely on a Lagrangian formulation<sup>16,17,19</sup>, but employ an implicit differentiation scheme instead. This has the advantage that we obtain, in addition to the excited state energy gradients, also the gradients of KS energies and wavefunctions. The latter may be exploited to compute nonadiabatic coupling matrix elements between different electronic states. We have implemented

the working equations within a plane wave/pseudopotential code<sup>20</sup> and we will demonstrate numerical accuracy and illustrate the convergence behaviour with respect to the number of MOs included in the active space for some prototypical test examples.

## II. THEORY

The linear response TDDFT eigenvalue problem can be written in Hermitian form as

$$\boldsymbol{\Omega}|\mathbf{F}_n\rangle = \omega_n^2|\mathbf{F}_n\rangle \quad , \quad (1)$$

where the response matrix  $\boldsymbol{\Omega}$  is defined as

$$\Omega_{ph\sigma,p'h'\sigma'} = \delta_{\sigma\sigma'}\delta_{pp'}\delta_{hh'}(\epsilon_{p\sigma} - \epsilon_{h\sigma})^2 + 2\sqrt{\epsilon_{p\sigma} - \epsilon_{h\sigma}}K_{ph\sigma,p'h'\sigma'}\sqrt{\epsilon_{p'\sigma} - \epsilon_{h'\sigma}} \quad , \quad (2)$$

with the coupling matrix

$$K_{ph\sigma,p'h'\sigma'} = \int d\mathbf{r} \int d\mathbf{r}' \psi_{p\sigma}(\mathbf{r})\psi_{h\sigma}(\mathbf{r})f_{\text{H,xc}}^{\sigma\sigma'}(\mathbf{r}, \mathbf{r}')\psi_{p'\sigma'}(\mathbf{r}')\psi_{h'\sigma'}(\mathbf{r}') \quad , \quad (3)$$

$\psi_{p\sigma}$  and  $\psi_{h\sigma}$  being the KS particle (unoccupied) and hole (occupied) molecular orbitals with spin  $\sigma$  corresponding to the KS energies  $\epsilon_{p\sigma}$  and  $\epsilon_{h\sigma}$ , respectively. The response kernel

$$f_{\text{H,xc}}^{\sigma\sigma'}(\mathbf{r}, \mathbf{r}') = \frac{1}{|\mathbf{r} - \mathbf{r}'|} + \delta(\mathbf{r} - \mathbf{r}')\frac{\delta^2 E_{\text{xc}}}{\delta \rho^\sigma(\mathbf{r})\delta \rho^{\sigma'}(\mathbf{r}')} \quad (4)$$

containing a Hartree term and an exchange-correlation term is given in the usual adiabatic approximation<sup>21</sup>, i.e. the exchange-correlation contribution is taken to be simply the second derivative of the static ground state exchange-correlation energy,  $E_{\text{xc}}$ , with respect to the spin density  $\rho^\sigma$ .

For the sake of simplicity, the following derivation is for singlet excitations only (extension to triplet excitations is straightforward). We shall therefore drop the spin index  $\sigma$ . The reduced (singlet) response matrix is given by

$$\Omega_{ph,p'h'} = \delta_{pp'}\delta_{hh'}(\epsilon_p - \epsilon_h)^2 + 4\sqrt{\epsilon_p - \epsilon_h}K_{ph,p'h'}\sqrt{\epsilon_{p'} - \epsilon_{h'}} \quad , \quad (5)$$

where

$$K_{ph,p'h'} = \int d\mathbf{r} \int d\mathbf{r}' \psi_p(\mathbf{r})\psi_h(\mathbf{r})f_{\text{H,xc}}(\mathbf{r}, \mathbf{r}')\psi_{p'}(\mathbf{r}')\psi_{h'}(\mathbf{r}') \quad , \quad (6)$$

and

$$f_{\text{H,xc}}(\mathbf{r}, \mathbf{r}') = \frac{1}{|\mathbf{r} - \mathbf{r}'|} + \delta(\mathbf{r} - \mathbf{r}')\frac{\delta^2 E_{\text{xc}}}{\delta \rho(\mathbf{r})^2} \quad . \quad (7)$$

Multiplying eq. (1) by  $\langle \mathbf{F}_n |$  from the left we obtain

$$\langle \mathbf{F}_n | \mathbf{\Omega} | \mathbf{F}_n \rangle = \omega_n^2 \quad . \quad (8)$$

Differentiation with respect to the nuclear coordinate  $R_\alpha$  ( $\alpha = 1, \dots, 3N$ ) for a molecule consisting of  $N$  atoms yields

$$\omega_n^\alpha = \frac{1}{2\omega_n} \langle \mathbf{F}_n | \mathbf{\Omega}^\alpha | \mathbf{F}_n \rangle = \frac{1}{2\omega_n} \sum_{ph} \sum_{p'h'} F_{ph}^{(n)} \Omega_{ph,p'h'}^\alpha F_{p'h'}^{(n)} \quad , \quad (9)$$

where we have used the short-hand notation  $\frac{df}{dR_\alpha} \equiv f^\alpha$ ; the  $F_{ph}^{(n)}$  are the components of the linear response eigenvector  $\mathbf{F}_n$ . Carrying out the differentiation of the response matrix, eq. (9) becomes

$$\begin{aligned} \omega_n^\alpha = & \frac{1}{\omega_n} \left[ \sum_{ph} (F_{ph}^{(n)})^2 (\epsilon_p^\alpha - \epsilon_h^\alpha) (\epsilon_p - \epsilon_h) \right. \\ & + 2 \int d\mathbf{r} \int d\mathbf{r}' \Gamma_1(\mathbf{r}) f_{\text{H,xc}}(\mathbf{r}, \mathbf{r}') \Gamma_2(\mathbf{r}') \\ & \left. + 2 \int d\mathbf{r} \Gamma_1(\mathbf{r}) \frac{\delta^3 E_{\text{xc}}}{\delta \rho(\mathbf{r})^3} \rho^\alpha(\mathbf{r}) \Gamma_1(\mathbf{r}) \right] \quad . \end{aligned} \quad (10)$$

Here we have defined the contracted densities

$$\Gamma_1(\mathbf{r}) = \sum_{ph} F_{ph}^{(n)} \sqrt{\epsilon_p - \epsilon_h} \Gamma_{ph}(\mathbf{r}) \quad (11)$$

and

$$\Gamma_2(\mathbf{r}) = \sum_{ph} F_{ph}^{(n)} \left[ \frac{\epsilon_p^\alpha - \epsilon_h^\alpha}{\sqrt{\epsilon_p - \epsilon_h}} \Gamma_{ph}(\mathbf{r}) + 2 \sqrt{\epsilon_p - \epsilon_h} \Gamma_{ph}^\alpha(\mathbf{r}) \right] \quad (12)$$

with

$$\Gamma_{ij}(\mathbf{r}) = \psi_i(\mathbf{r}) \psi_j(\mathbf{r}) \quad (13)$$

In order to compute the excitation energy gradient (eq. (10)), we require the nuclear derivatives of KS orbital energies and wavefunctions,  $\epsilon_i^\alpha$  and  $\psi_i^\alpha$  ( $i = p, h$ ). These can be obtained using an implicit differentiation scheme as follows. We start by writing down the KS equations in matrix form

$$F_{ij} \equiv H_{ij} - \epsilon_i \delta_{ij} = 0 \quad . \quad (14)$$

For the full differential of  $F_{ij}$  we have

$$dF_{ij} = \left( \frac{\partial H_{ij}}{\partial R_\alpha} - \epsilon_i^\alpha \delta_{ij} \right) dR_\alpha + \sum_k \int d\mathbf{r} H_{ij}^k \delta \psi_k(\mathbf{r}) = 0 \quad , \quad (15)$$

where  $H_{ij}^k \equiv \frac{\delta H_{ij}}{\delta \psi_k(\mathbf{r})}$ . Division by  $dR_\alpha$  yields

$$\frac{\partial H_{ij}}{\partial R_\alpha} - \epsilon_i^\alpha \delta_{ij} = - \sum_k \int d\mathbf{r} H_{ij}^k \psi_k^\alpha(\mathbf{r}) = - \sum_k \int d\mathbf{r} \int d\mathbf{r}' H_{ij}^k \delta(\mathbf{r} - \mathbf{r}') \psi_k^\alpha(\mathbf{r}') \quad . \quad (16)$$

On the rhs of eq. (16) we have inserted a delta function, which we now express in terms of KS orbitals

$$\delta(\mathbf{r} - \mathbf{r}') = \sum_l \psi_l(\mathbf{r}) \psi_l(\mathbf{r}') \quad . \quad (17)$$

Thus eq. (16) becomes

$$\frac{\partial H_{ij}}{\partial R_\alpha} - \epsilon_i^\alpha \delta_{ij} = - \sum_{kl} H_{ij}^{kl} \psi_k^{\alpha l} \quad , \quad (18)$$

where

$$\begin{aligned} H_{ij}^{kl} &\equiv \int d\mathbf{r} H_{ij}^k \psi_l(\mathbf{r}) \\ &= (\delta_{ik} \delta_{lj} + \delta_{jk} \delta_{li}) \epsilon_l + 2n_k \int d\mathbf{r} \int d\mathbf{r}' \Gamma_{kl}(\mathbf{r}) f_{\text{H,xc}}(\mathbf{r}, \mathbf{r}') \Gamma_{ij}(\mathbf{r}') \quad , \end{aligned} \quad (19)$$

and

$$\psi_k^{\alpha l} \equiv \int d\mathbf{r} \psi_l(\mathbf{r}) \psi_k^\alpha(\mathbf{r}) \quad , \quad (20)$$

$n_k$  being the number of electrons occupying orbital  $k$ .

Exploiting the symmetry of the nonadiabatic coupling matrix elements (20), i.e.  $\psi_l^{\alpha k} = -\psi_k^{\alpha l}$  and therefore  $\psi_l^{\alpha l} = 0$ , eq. (18) can be rewritten as

$$\frac{\partial H_{ij}}{\partial R_\alpha} = \sum_{l < k} D_{ij}^{lk} \psi_k^{\alpha l} \quad , (i < j) \quad (21)$$

and for the diagonal terms ( $i = j$ )

$$\epsilon_i^\alpha = \frac{\partial H_{ii}}{\partial R_\alpha} - \sum_{k < l} D_{ii}^{kl} \psi_k^{\alpha l} \quad . \quad (22)$$

where

$$D_{ij}^{lk} = H_{ij}^{lk} - H_{ij}^{kl} = (\delta_{il} \delta_{kj} + \delta_{ik} \delta_{lj}) (\epsilon_k - \epsilon_l) + 2(n_k - n_l) K_{ij,lk} \quad (23)$$

With the definition (23) eq. (21) becomes

$$\frac{\partial H_{hp}}{\partial R_\alpha} = \sum_{p'h'} ((\epsilon_{p'} - \epsilon_{h'}) \delta_{pp'} \delta_{hh'} + 4K_{p'h',ph}) \psi_{h'}^{\alpha p'} \quad (24)$$

for particle-hole states, and

$$\frac{\partial H_{ij}}{\partial R_\alpha} = 4 \sum_{ph} K_{ij,ph} \psi_h^{\alpha p} + (\epsilon_i - \epsilon_j) \psi_i^{\alpha j} \quad , (i < j, ij \ni ph) \quad (25)$$

for all remaining combinations. Eq. (25) allows us to express the nonadiabatic coupling elements between non-particle-hole states analytically as

$$\psi_i^{\alpha j} = \frac{\frac{\partial H_{ij}}{\partial R_\alpha} + 4 \sum_{ph} K_{ij,ph} \psi_h^{\alpha p}}{(\epsilon_i - \epsilon_j)} , (i < j, ij \ni ph) \quad (26)$$

The system of linear equations (24) is first solved for the particle-hole nonadiabatic coupling elements  $\psi_p^{\alpha h}$ , which are then inserted into eq. (26) to obtain the remaining, non-particle-hole, elements. The second term in the numerator of eq. (26) is most conveniently evaluated by introducing the contracted density

$$\Gamma_3(\mathbf{r}) = \sum_{ph} \psi_p(\mathbf{r}) \psi_h(\mathbf{r}) \psi_h^{\alpha p} \quad (27)$$

Then

$$\sum_{ph} K_{ij,ph} \psi_p^{\alpha h} = \int d\mathbf{r} \int d\mathbf{r}' \Gamma_3(\mathbf{r}) f_{H,xc}(\mathbf{r}, \mathbf{r}') \psi_i(\mathbf{r}') \psi_j(\mathbf{r}') \equiv K'_{ij} \quad (28)$$

Thus eq. (26) becomes

$$\psi_j^{\alpha i} = \frac{\frac{\partial H_{ij}}{\partial R_\alpha} + 4K'_{ij}}{(\epsilon_i - \epsilon_j)} , (i < j, ij \ni ph) \quad (29)$$

Similarly the KS orbital energy gradients can now be obtained from the simplified eq. (22)

$$\epsilon_i^\alpha = \frac{\partial H_{ii}}{\partial R_\alpha} + 4K'_{ii} . \quad (30)$$

Finally, the nuclear derivative of the KS orbital wavefunction is recovered by unfolding the nonadiabatic couplings

$$\psi_k^\alpha(\mathbf{r}) = \sum_l \psi_l(\mathbf{r}) \psi_k^{\alpha l} . \quad (31)$$

Equations (1)–(31) have been implemented with periodic boundary conditions using a plane wave expansion of the KS MOs at the  $\Gamma$  point of the Brillouin zone. By making use of the periodic boundary conditions, the generalized densities  $\Gamma_1$ ,  $\Gamma_2$ ,  $\Gamma_3$  and  $\Gamma_{ij}$  can be expanded in reciprocal space via the three-dimensional Fourier transform, e.g.

$$\Gamma_1(\mathbf{r}) = \sum_{\mathbf{G}} \Gamma_1(\mathbf{G}) \exp(i\mathbf{Gr}) \quad (32)$$

where  $\mathbf{G}$  is the vector of the reciprocal lattice. The Hartree part of the matrix element  $\int d\mathbf{r} \int d\mathbf{r}' \Gamma_1(\mathbf{r}) f_{H,xc}(\mathbf{r}, \mathbf{r}') \Gamma_2(\mathbf{r}')$  and  $\int d\mathbf{r} \int d\mathbf{r}' \Gamma_{kl}(\mathbf{r}) f_{H,xc}(\mathbf{r}, \mathbf{r}') \Gamma_{ij}(\mathbf{r}')$  which enter the key equations (10) and (19), respectively, can be readily computed in reciprocal space, e.g.

$$\int d\mathbf{r} \int d\mathbf{r}' \Gamma_1(\mathbf{r}) \frac{1}{|\mathbf{r} - \mathbf{r}'|} \Gamma_2(\mathbf{r}') = \Omega \sum_{\mathbf{G} \neq 0} \frac{2\pi}{G^2} \Gamma_1(\mathbf{G}) \Gamma_2(\mathbf{G}) \quad (33)$$

whereas the exchange-correlation parts of the matrix elements are calculated via direct numerical integration over grid in coordinate space.

### III. TEST RESULTS

To illustrate the performance and the convergence behaviour of our method, we have computed nuclear gradients of the first excited state energies of  $H_2$  and  $N_2$ . The calculations were performed using our implementation of the formalism presented here in the CPMD package<sup>20</sup>. All the systems were treated employing periodic boundary conditions and the molecular orbitals were expanded in plane waves at the  $\Gamma$  point of the Brillouin zone. We used Troullier-Martins normconserving pseudopotentials<sup>22</sup>. The excitation energies and nuclear gradients were computed within the adiabatic local density approximation<sup>23</sup> to the linear response exchange-correlation kernel.

The central idea underlying the present active space approach originates from the observation that excitation energies for a large number of electronic transitions exhibit only a minor dependence on the size of the response matrix (2). This is illustrated in Table 1 for the  $3\sigma_g \rightarrow 1\pi_g$  transition of  $N_2$ . A simple two-state HOMO–LUMO response calculation is seen to give an excitation energy which is less than 0.2 eV away from an extended treatment including all 5 occupied and 100 virtual MOs. Generally, such behaviour is to be expected for excitations which can be characterized by only a few low-lying one-electron transitions without higher-lying continuum states mixing in.

In the following, we shall discuss the active space dependence of the excitation energy gradients and the KS orbital energy gradients. The upper panel of Fig. 1 displays the completeness of the active space as a function of the number of virtual KS orbitals included in the space. The integral

$$C(N) = \int d\mathbf{r} \sum_{i=1}^N \psi_i(\mathbf{r})\psi_i(0) \quad (34)$$

was used as a measure of completeness of the active space. It becomes unity when the active space of KS orbitals is complete, i.e. when the total number of the KS orbitals (virtual and occupied) equals the number of plane waves used to solve the KS equations. The total number of plane waves is 925 for the 6 a.u. cubic box and 40 Ry plane wave cutoff. With 450 virtual orbitals included the active space is almost complete and the value of the

integral (34) deviates from unity by approximately  $10^{-3}$  which is already comparable with the accuracy of the numerical integration. The lower panel of Fig. 1 shows the absolute deviation of the analytic derivatives from the respective finite difference values for the the first singlet excitation energy,  $\omega_1$ , as well as the HOMO and LUMO KS orbital energies,  $\epsilon_1$  and  $\epsilon_2$ , of  $\text{H}_2$  at a bond length of 1.0 a.u. as a function of the number of virtual KS orbitals included in the active space. The absolute deviation in analytical gradients vanishes rapidly as the number of virtual orbitals is increased and the errors in the analytical gradients of different states generally show the same patterns in the dependence upon the number of virtual orbitals included in the active space.

Fig. 2 shows the absolute deviation of the analytical derivative from the respective finite difference value as a function of the size of the active space for the first three KS orbital energies  $\epsilon_i$  ( $i = 1, 2, 3$ ) as well as the lowest response matrix eigenvalue  $\omega_1$  of the  $\text{N}_2$  molecule. The errors of the analytical gradients are seen to decrease rapidly as the number of orbitals included in the active space approaches the number of plane wave basis functions (in this case 925 plane waves). For the largest active space the deviations of all energies are of the order of  $10^{-3}$  or smaller. At this point, the accuracy of the analytical derivatives is hard to assess because the finite difference reference values are also subject to numerical errors. We have further checked whether the excited state gradients are invariant under translation. The translational contribution to the excitation energy gradient is found to decrease rapidly as the active space increases. Interestingly, the underlying ground state calculation exhibits a significantly larger translational error than the excitation energy.

To test the practical value of our derivatives, we have performed geometry optimizations of  $\text{N}_2$  in the first excited state ( $8 \times 5.6 \times 5.6$  a.u. box, 40 Ry plane-wave cutoff, i.e. 600 basis functions). When we include only 100 virtual orbitals in the active space, we obtain a bond length of 2.44 a.u., which deviates by 0.02 a.u. from the value of 2.42 a.u. determined by a series of single point energy calculations. Upon increasing the number of virtual states to 200, the optimized bond length comes out as 2.42 a.u., correct to two decimal places. Our test calculations illustrate how the size of the active space may be adjusted to achieve any desired level of accuracy. For many practical purposes it will be sufficient to work with a reduced active space which is significantly smaller than the total number of basis functions.

The situation is different in the case of molecular dynamics simulations, where the nuclear forces need to be essentially exact derivatives of the potential in order to maintain conser-

vation of energy. Although we have already carried out test excited state MD simulations for diatomic molecules, those results do not offer any additional insight into the general performance and convergence pattern of our method. We have not yet applied the formalism presented here to perform more realistic excited state MD simulations of polyatomic molecules, because our current implementation does not yet make use of more efficient iterative techniques, such as Lanczos algorithm or related schemes<sup>24</sup>, to solve the response eigenvalue problem (1). These numerical techniques, however, are standard and we plan to exploit them in future implementations. The scope of this article is merely the presentation of the formalism and the analysis of the convergence behaviour with respect to the choice of the active space.

We would like to emphasize, however, that the method described here is capable of providing additional information beyond excited state energy gradients. Fig. 3 shows, for instance, the nonadiabatic coupling strength between the second and third KS orbitals,  $\psi_2$  and  $\psi_3$ , for the H<sub>2</sub> molecule as a function of its bond length. The nonadiabatic coupling values obtained from eqn (29) exhibit a singularity at the crossing point between the two KS orbital energies, as one would expect due to the KS energy difference in the denominator. This feature of our formalism may be exploited in future applications of TDDFT beyond the Born-Oppenheimer approximation.

#### IV. CONCLUSIONS

We have developed and implemented an novel, alternative formalism to calculate analytical nuclear forces for TDDFT excited states within a plane wave/pseudopotential framework. In addition to the excited state energy gradient, our method also provides molecular orbital wavefunction as well as energy derivatives at a small computational overhead compared to the vertical excitation energies. The latter may, for instance be employed as a powerful tool for understanding and interpreting various chemical phenomena such as molecular structures and reactivities<sup>25</sup>. A fundamental quantity in the present formalism are the nonadiabatic coupling elements in the molecular orbital basis which are obtained as direct solutions of a system of linear equations. These matrix elements may provide the basis for the calculation of nonadiabatic couplings between the many-electron adiabatic wavefunctions. Trial calculations on the prototypical test molecules H<sub>2</sub> and N<sub>2</sub> demonstrate that our implementation

reproduces the exact gradients when the number of molecular orbital included in the active space approaches the number of plane wave basis functions. Excited state geometry optimization of  $N_2$  using different active spaces show that for many practical purposes it will be sufficient to work within a relatively small active space. The size of the latter may be tuned to achieve any desired level of accuracy.

### **Acknowledgments**

We are grateful to J. Hutter and F. Furche for helpful discussions.

## APPENDIX A: CALCULATION OF $\frac{\partial H_{ij}}{\partial R}$ IN PLANE WAVES

The matrix elements of the derivatives of the KS Hamiltonian are required for the calculations of the KS molecular orbitals gradients. Since the kinetic and exchange-correlation energies do not depend directly upon the atomic positions, the matrix element of the derivative becomes (local/nonlocal pseudopotential and electrostatic interaction contributions):

$$\frac{\partial H_{ij}}{\partial R_I} = \frac{\partial}{\partial R} H_{ij}^{pp,local} + \frac{\partial}{\partial R} H_{ij}^{pp,nonlocal} + \frac{\partial}{\partial R} H_{ij}^{es} \quad (A1)$$

All these matrix elements are computed in reciprocal space. The matrix element of the derivative of the local pseudopotential has the following form

$$\frac{\partial}{\partial \mathbf{R}_I} H_{ij}^{pp,local} = -\Omega \sum_{\mathbf{G}} i \mathbf{G} V_{local}^I(\mathbf{G}) S_I(\mathbf{G}) \Gamma_{ij}(\mathbf{G}) \quad (A2)$$

where  $\mathbf{R}_I$  denotes the atomic position and the structure factor  $S_I = \exp(i\mathbf{G}\mathbf{R}_I)$  of nuclei  $I$ ,  $\Gamma_{ij}(\mathbf{G})$  is the three-dimensional Fourier transform of the contracted density (13). The nonlocal pseudopotential contribution is

$$\frac{\partial}{\partial \mathbf{R}_I} H_{ij}^{pp,nonlocal} = \sum_{\mu\nu \in I} \left[ \left( \frac{\partial F_{I,i}^\mu}{\partial \mathbf{R}_I} \right)^* h_{\mu\nu}^I F_{I,j}^\nu + (F_{I,i}^\mu)^* h_{\mu\nu}^I \frac{\partial F_{I,j}^\nu}{\partial \mathbf{R}_I} \right], \quad (A3)$$

where the contribution from the projector derivative  $\frac{\partial F_{I,i}^\mu}{\partial \mathbf{R}_I}$  is calculated in the standard way<sup>26</sup>.

The contribution from the electrostatic energy is computed in the form

$$\frac{\partial}{\partial \mathbf{R}_I} H_{ij}^{es} = -\Omega \sum_{\mathbf{G} \neq 0} i \frac{\mathbf{G}}{G^2} \Gamma_{ij}^*(\mathbf{G}) n_c^I(\mathbf{G}) S_I(\mathbf{G}) \quad (A4)$$

where  $n_c^I(\mathbf{G})$  is the gaussian core charge distribution for nuclei  $I$  in reciprocal space.

## APPENDIX B: THIRD FUNCTIONAL DERIVATIVES OF THE EXCHANGE-CORRELATION FUNCTIONAL

### 1. Third derivative of Vosko-Wilk-Nusair correlation

$$E_c = \int \rho \epsilon_c d\mathbf{r} \quad , \quad (B1)$$

where

$$\epsilon_c = A \left\{ \ln \frac{x^2}{X(x)} + \frac{2b}{Q} \tan^{-1} \frac{Q}{X'(x)} - \frac{bx_0}{X(x_0)} \left[ \ln \frac{(x-x_0)^2}{X(x)} + \frac{2X'(x_0)}{Q} \tan^{-1} \frac{Q}{X'(x)} \right] \right\} \quad (\text{B2})$$

with  $x = \sqrt{r_s}$ ,  $r_s = (\frac{3}{4\pi\rho})^{\frac{1}{3}}$ ,  $X(x) = x^2 + bx + c$ ,  $X'(x) \equiv \frac{dX}{dx} = 2x + b$ ,  $Q = \sqrt{4c - b^2}$ ,  $A = 0.0310907$ ,  $b = 3.72744$ ,  $c = 12.9352$ ,  $x_0 = -0.10498$ .

$$\frac{\delta E_c}{\delta \rho} = \epsilon_c + \rho \frac{\partial \epsilon_c}{\partial \rho} \quad (\text{B3})$$

where

$$\frac{\partial \epsilon_c}{\partial \rho} = \frac{\partial x}{\partial \rho} \frac{\partial \epsilon_c}{\partial x} = -\frac{x}{6\rho} \frac{\partial \epsilon_c}{\partial x} \quad (\text{B4})$$

and

$$\frac{\partial \epsilon_c}{\partial x} = A \left\{ \frac{2}{x} - \frac{X}{X'} - \frac{4b}{X'^2 + Q^2} - \frac{bx_0}{X(x_0)} \left[ \frac{2}{x-x_0} - \frac{X}{X'} - \frac{4X'(x_0)}{X'^2 + Q^2} \right] \right\} \quad (\text{B5})$$

$$\frac{\delta^2 E_c}{\delta \rho^2} = 2 \frac{\partial \epsilon_c}{\partial \rho} + \rho \frac{\partial^2 \epsilon_c}{\partial \rho^2} \quad (\text{B6})$$

with

$$\frac{\partial^2 \epsilon_c}{\partial \rho^2} = \frac{\partial}{\partial \rho} \left( -\frac{1}{6} \frac{x}{\rho} \frac{\partial \epsilon_c}{\partial x} \right) = -\frac{1}{6} \left[ \left( \frac{\partial}{\partial \rho} \frac{x}{\rho} \right) \frac{\partial \epsilon_c}{\partial x} + \frac{x}{\rho} \left( \frac{\partial}{\partial \rho} \frac{\partial \epsilon_c}{\partial x} \right) \right] \quad (\text{B7})$$

$$= \frac{7}{36} \frac{x}{\rho^2} \frac{\partial \epsilon_c}{\partial x} + \frac{1}{36} \frac{x^2}{\rho^2} \frac{\partial^2 \epsilon_c}{\partial x^2} \quad (\text{B8})$$

Using relation (B4), eqn (B7) can be rewritten as

$$\frac{\partial^2 \epsilon_c}{\partial \rho^2} = -\frac{7}{6} \frac{1}{\rho} \frac{\partial \epsilon_c}{\partial \rho} + \frac{1}{36} \frac{x^2}{\rho^2} \frac{\partial^2 \epsilon_c}{\partial x^2} \quad (\text{B9})$$

and thus eqn (B6) becomes

$$\frac{\delta^2 E_c}{\delta \rho^2} = \frac{5}{6} \frac{\partial \epsilon_c}{\partial \rho} + \frac{1}{36} \frac{x^2}{\rho} \frac{\partial^2 \epsilon_c}{\partial x^2} \quad (\text{B10})$$

where

$$\frac{\partial^2 \epsilon_c}{\partial x^2} = A \left\{ -\frac{2}{x^2} - \frac{2}{X} + \left( \frac{X'}{X} \right)^2 + \frac{16bX'}{(X'^2 + Q^2)^2} \right\} \quad (\text{B11})$$

$$+ \frac{bx_0}{X(x_0)} \left[ \frac{2}{(x-x_0)^2} + \frac{2}{X} - \left( \frac{X'}{X} \right)^2 - \frac{16X'(x_0)X'(x)}{(X'^2 + Q^2)^2} \right] \quad (\text{B12})$$

$$\frac{\delta^3 E_c}{\delta \rho^3} = 3 \frac{\partial^2 \epsilon_c}{\partial \rho^2} + \rho \frac{\partial^3 \epsilon_c}{\partial \rho^3} \quad (\text{B13})$$

$$= -\frac{1}{36} \left[ 35 \frac{\partial \epsilon_c}{\partial \rho} + \frac{1}{2} \frac{x^2}{\rho} \frac{\partial^2 \epsilon_c}{\partial x^2} + \frac{1}{6} \frac{x^3}{\rho} \frac{\partial^3 \epsilon_c}{\partial x^3} \right] \quad (\text{B14})$$

with

$$\begin{aligned} \frac{\partial^3 \epsilon_c}{\partial x^3} = & A \left\{ \frac{4}{x^3} + 6 \frac{X'}{X^2} - 2 \left( \frac{X'}{X} \right)^3 + \frac{32b}{(X'^2 + Q^2)^2} \left[ 1 - \frac{4X'^2}{X'^2 + Q^2} \right] \right. \\ & \left. + \frac{bx_0}{X(x_0)} \left[ -\frac{4}{(x - x_0)^3} - 6 \frac{X'}{X^2} + 2 \left( \frac{X'}{X} \right)^3 - \frac{32X'(x_0)}{(X'^2 + Q^2)^2} \left[ 1 - \frac{4X'^2}{X'^2 + Q^2} \right] \right] \right\} \end{aligned} \quad (\text{B15})$$

One arrives at eqn (B14) by substituting eqn (B9) into eqn (B13). For instance,

$$\frac{\partial^3 \epsilon_c}{\partial \rho^3} = \frac{\partial}{\partial \rho} \left[ -\frac{7}{6} \frac{1}{\rho} \frac{\partial \epsilon_c}{\partial \rho} + \frac{1}{36} \frac{x^2}{\rho^2} \frac{\partial^2 \epsilon_c}{\partial x^2} \right] \quad (\text{B16})$$

$$= -\frac{7}{6} \frac{1}{\rho} \left( \frac{\partial^2 \epsilon_c}{\partial \rho^2} - \frac{1}{\rho} \frac{\partial \epsilon_c}{\partial \rho} \right) - \frac{1}{108} \frac{x^2}{\rho^3} \left( 7 \frac{\partial^2 \epsilon_c}{\partial x^2} + \frac{1}{2} x \frac{\partial^3 \epsilon_c}{\partial x^3} \right) \quad (\text{B17})$$

where we have used

$$\frac{\partial}{\partial \rho} \left( \frac{x}{\rho} \right)^2 = -\frac{7}{3} \frac{x^2}{\rho^3} \quad (\text{B18})$$

## 2. Third derivative of Slater exchange

$$E_x = \int \rho \epsilon_x d\mathbf{r} \quad , \quad (\text{B19})$$

where

$$\epsilon_x = C \alpha \rho^{\frac{1}{3}} , \quad C = -\frac{9}{8} \left( \frac{3}{\pi} \right)^{\frac{1}{3}} , \quad \alpha = \frac{2}{3} \quad (\text{B20})$$

The third derivatives can be readily computed

$$\frac{\partial^3 E_x}{\partial \rho^3} = -C \alpha^4 \rho^{-\alpha-1} \quad (\text{B21})$$

---

<sup>1</sup> E. Runge and E. K. U. Gross, Phys. Rev. Lett. **52**, 997 (1984).

<sup>2</sup> M. E. Casida, in *Recent Advances in Density-Functional Methods*, edited by D. P. Chong, page 155 (World Scientific, Singapore, 1995).

<sup>3</sup> R. Bauernschmitt and R. Ahlrichs, Chem. Phys. Lett. **256**, 454 (1996).

<sup>4</sup> N. T. Maitra, K. Burke, H. Appel, E. K. U. Gross, and R. van Leeuwen, in *Reviews in Modern Quantum Chemistry: A Celebration of the Contributions of R. G. Parr*, edited by K. D. Sen, volume 2, page 1186 (World-Scientific, Singapore, 2002).

<sup>5</sup> D. J. Tozer and N. C. Handy, Phys. Chem. Chem. Phys. **2**, 2117 (2000).

<sup>6</sup> L. Bernasconi, M. Sprik, and J. Hutter, Chem. Phys. Lett. **394**, 141 (2004).

<sup>7</sup> A. Dreuw, J. L. Weisman, and M. Head-Gordon, J. Chem. Phys. **119**, 2943 (2003).

<sup>8</sup> M. E. Casida, F. Gutierrez, J. Guan, F. Gadea, D. Salahub, and J.-P. Daudey, J. Chem. Phys. **113**, 7062 (2000).

<sup>9</sup> S. Hirata and M. Head-Gordon, Chem. Phys. Lett. **302**, 375 (1999).

<sup>10</sup> H. Appel, E. K. U. Gross, and K. Burke, Phys. Rev. Lett. **90**, 043005 (2003).

<sup>11</sup> P. R. T. Schipper, O. V. Gritsenko, S. J. A. van Gisbergen, and E. J. Baerends, J. Chem. Phys. **112**, 1344 (2000).

<sup>12</sup> H. H. Neinze, A. Görling, and N. Rösch, J. Chem. Phys. **113**, 2088 (2000).

<sup>13</sup> D. J. Tozer and N. C. Handy, J. Chem. Phys. **109**, 10180 (1998).

<sup>14</sup> C. van Caillie and R. D. Amos, Chem. Phys. Lett. **308**, 249 (1999).

<sup>15</sup> C. van Caillie and R. D. Amos, Chem. Phys. Lett. **317**, 159 (2000).

<sup>16</sup> F. Furche and R. Ahlrichs, J. Chem. Phys. **117**, 7433 (2002).

<sup>17</sup> J. Hutter, J. Chem. Phys. **118**, 3928 (2003).

<sup>18</sup> N. L. Doltsinis and M. Sprik, Chem. Phys. Lett. **330**, 563 (2000).

<sup>19</sup> E. R. Bittner and D. S. Kosov, J. Chem. Phys. **110**, 6645 (1999).

<sup>20</sup> CPMD 3.4: J. Hutter, P. Ballone, M. Bernasconi, P. Focher, E. Fois, S. Goedecker, D. Marx, M. Parrinello, and M. Tuckerman; MPI für Festkörperforschung, Stuttgart and IBM Zurich Research Laboratory.

<sup>21</sup> E. K. U. Gross and W. Kohn, Adv. Quant. Chem. **21**, 255 (1990).

<sup>22</sup> N. Troullier and J. L. Martins, Phys. Rev. B **43**, 1993 (1991).

<sup>23</sup> M. Petersilka, U. J. Grossmann, and E. K. U. Gross, Phys. Rev. Lett. **76**, 1212 (1996).

<sup>24</sup> R. E. Stratmann, G. E. Scuseria, and M. Frisch, J. Chem. Phys. **109**, 8218 (1998).

<sup>25</sup> Y. Yamaguchi, R. B. Remington, J. F. Gaw, H. F. Schaefer III, and G. Frenking, Chem. Phys. **180**, 55 (1994).

<sup>26</sup> D. Marx and J. Hutter, in *Modern Methods and Algorithms of Quantum Chemistry*, edited by J. Grotendorst (NIC, Jülich, 2000), for downloads see  
<http://www.theochem.ruhr-uni-bochum.de/go/cprev.html>.

active space	$\Delta E_{\text{KS}}$	1o/1v	5o/1v	5o/5v	5o/50v	5o/100v
exc. energy	8.39	9.47	9.40	9.40	9.33	9.29

TABLE I: Dependence of N<sub>2</sub> TDLDA excitation energy (<sup>1</sup> $\Pi_g$ , 3 $\sigma_g$   $\rightarrow$  1 $\pi_g$ ) in eV using plane waves (p.w.) with a 70 Ry cutoff in a 10  $a_0$  periodic box on the number of occupied (o) and virtual (v) Kohn-Sham orbitals included in the active space.  $\Delta E_{\text{KS}}$  is the unperturbed Kohn-Sham energy difference.

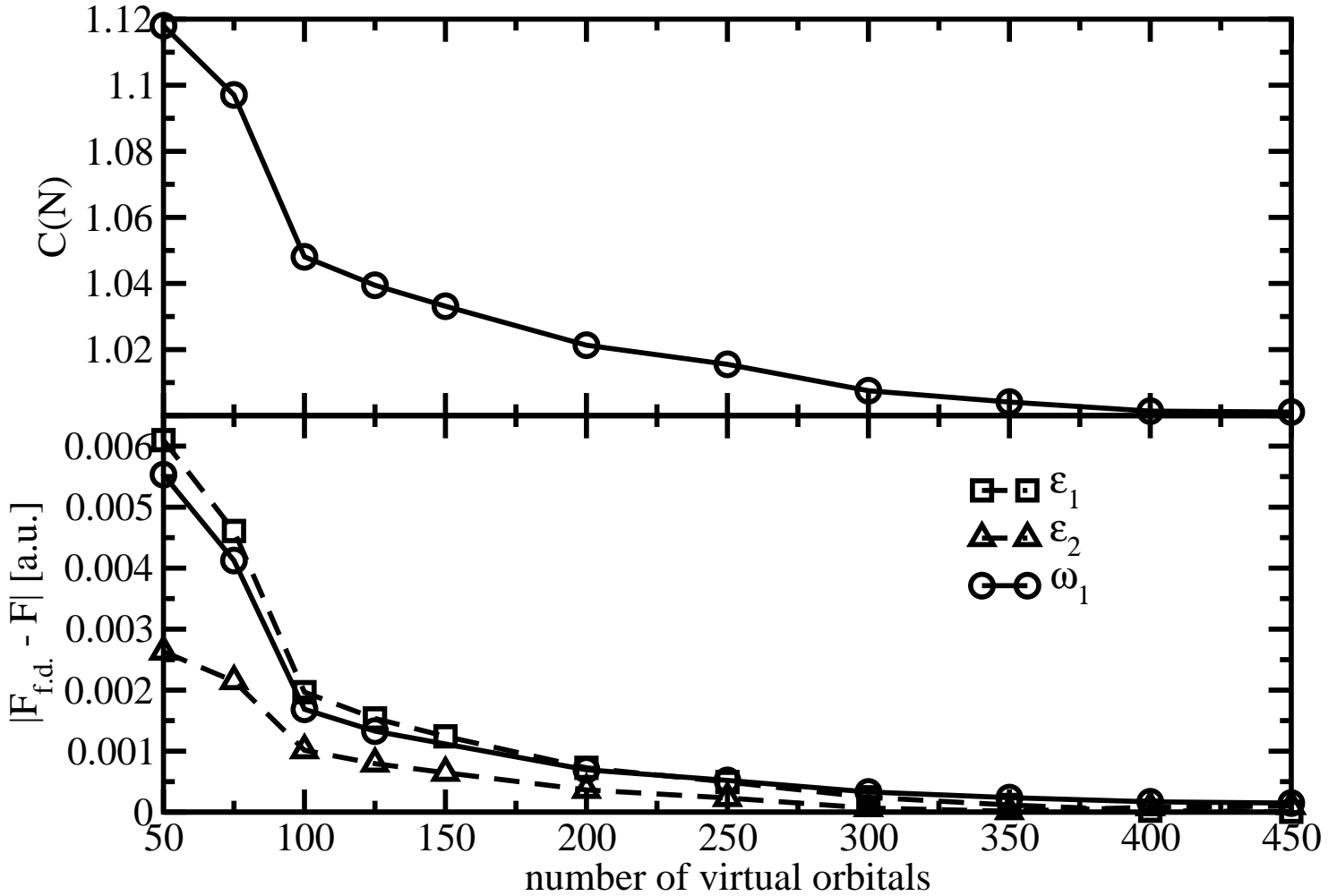


FIG. 1: (a) The integral (34) as a function of the number of virtual orbitals included in the active space. (b) Absolute deviation of finite difference and analytic derivatives of the Kohn-Sham HOMO and LUMO energies of  $H_2$  at a bond length of 1.0 a.u. as a function of the number of virtual Kohn-Sham orbitals included in the active space. (c) Absolute deviation of finite difference and analytic derivatives of the first singlet excitation energy of  $H_2$  at a bond length of 1.0 a.u. as a function of the number of virtual Kohn-Sham orbitals included in the active space. The calculations were carried out in a cubix box of length 6 a.u. with periodic boundary conditions and a plane wave cutoff of 40 Ry.

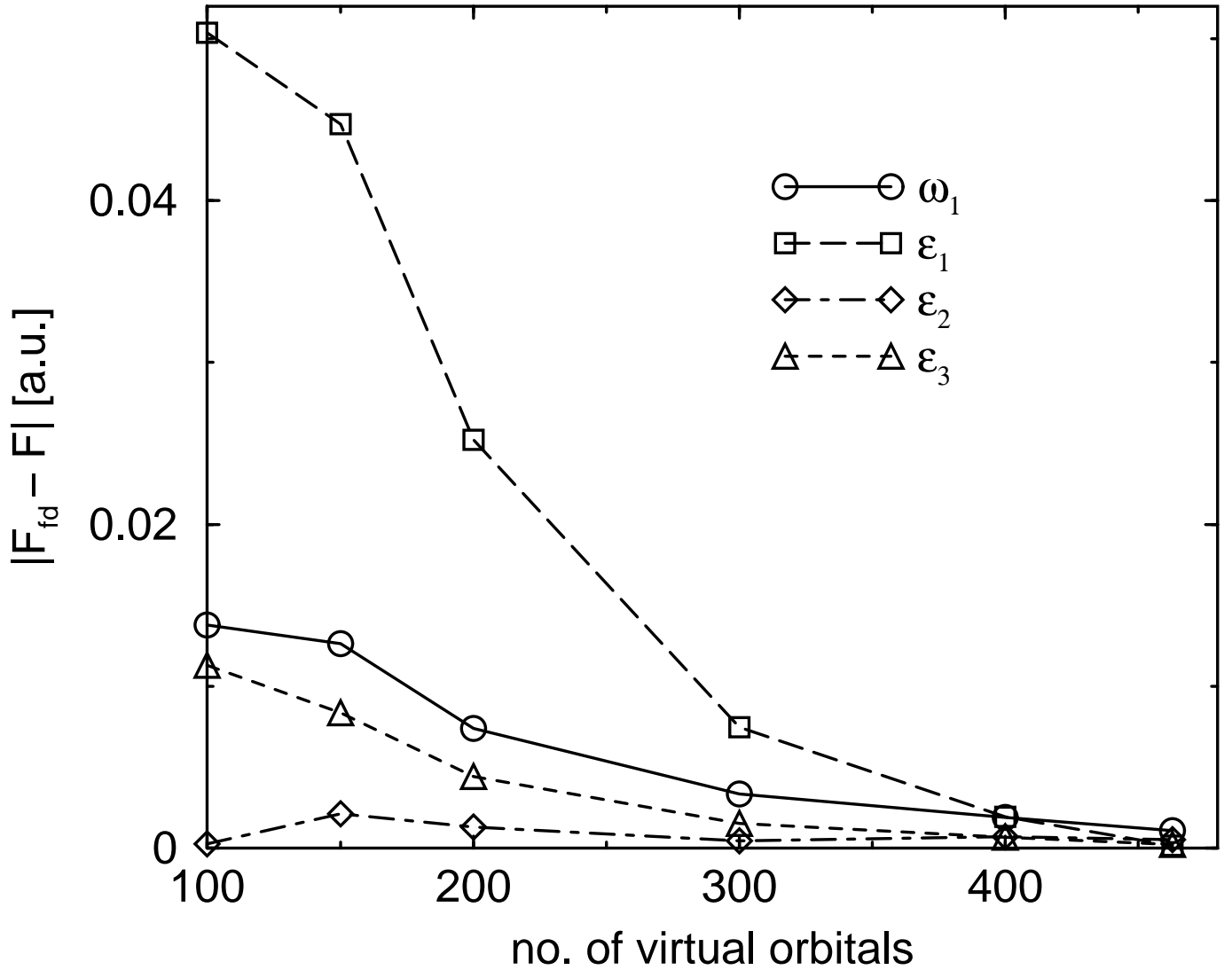


FIG. 2: Absolute deviation of the analytic derivatives from the respective finite difference values for the the first singlet excitation energy,  $\omega_1$ , as well as the three lowest KS orbital energies,  $\epsilon_i$  ( $i = 1, 2, 3$ ), of  $\text{N}_2$  at a bond length of 2.0 a.u. as a function of the number of virtual Kohn-Sham orbitals included in the active space. The calculations were carried out in a cubix box of length 6 a.u. with periodic boundary conditions and a plane wave cutoff of 40 Ry.

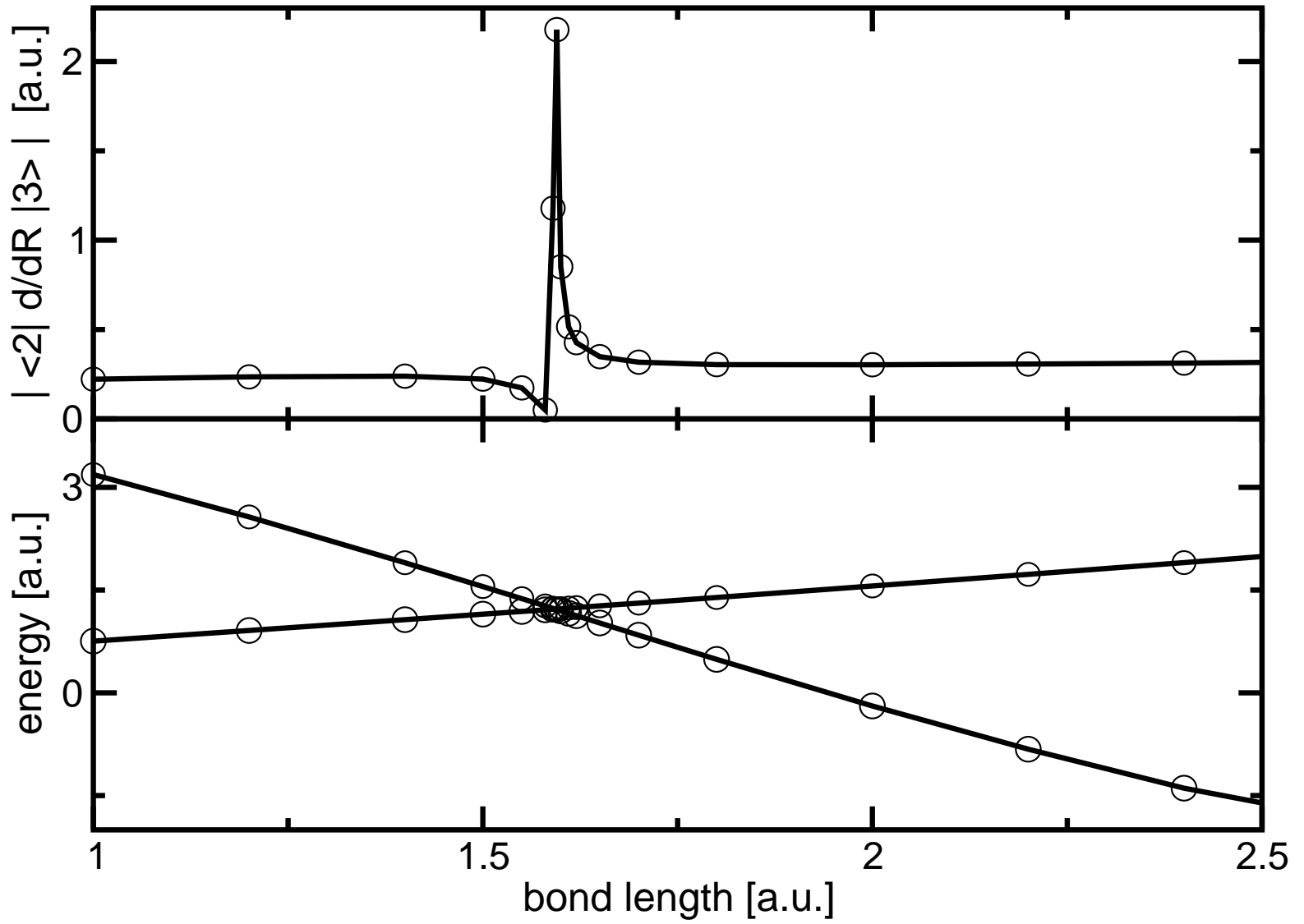


FIG. 3: Upper panel: Absolute value of the nonadiabatic coupling matrix element between the KS orbitals  $\psi_2$  and  $\psi_3$  along the molecular axis of  $\text{H}_2$  as a function of the bond length. Lower panel: KS orbital energies,  $\epsilon_2$  and  $\epsilon_3$  of  $\text{H}_2$  as a function of bond length. The calculations were carried out in a periodic orthorhombic box of size  $8 \times 5.6 \times 5.6$  a.u.<sup>3</sup> using a plane wave cutoff of 40 Ry.